Determining Characteristic Scales for the Dynamics and Geometry of Sandy Bedforms

B. McElroy & D. Mohrig
Jackson School of Geosciences, University of Texas, Austin, Texas, USA

A. Blom
Delft University of Technology, Environmental Fluid Mechanics, Delft, The Netherlands

ABSTRACT: With advent of the ability to collect abundant, high resolution, acoustically derived bed topography, comes the necessity to develop robust, computationally objective methods for assessing the character and evolution of sandy bedforms. We present a set of measures to summarize the following attributes for a train of bedforms: characteristic height, characteristic length, characteristic velocity, and characteristic deformation. While height and length are bulk geometric statistics that can be described with one bed field realization, velocity and deformation are dynamic aspects of the system that require multiple realizations of the bed elevation field. Using data collected from the North Loup River, Nebraska, USA and from flume experiments, we demonstrate how these four properties of a bed profile can be defined by the roughness function and cross-correlation of the active topography. These measures can be used to compare the states and behaviors of river bottoms across scales.

1 CONTEXT

Models and observations of sandy river bed evolution predict and verify, respectively, that the internal dynamics of sandy transport systems result in complex bed geometries and behaviors. Simplifying the system into a set of fundamental scales is a necessary step for comparing rivers, models, and laboratory experiments. Much work has been done on this topic, and recreating an appropriate bibliography is beyond the scope of this extended abstract. Suffice it to say that the papers and authors that have had a major influence on this work are, Nordin (1971), Nikora and others (1997), Hino (1968), and Jerolmack and Mohrig (2005a, 2005b).

These fundamental descriptors, or characteristic scales, should be determined in a robust and objective method such that many types of systems can be compared from observations of many workers. This can be accomplished by employing a set of measures based on numeric analysis of bed topography as continuous elevation fields. Although, there are quantifications that can be made by determining the set of discrete bedforms that comprise a bed, they are unavoidably subjective. This is typically due to the requirement of a threshold necessary to distinguish small elements from the larger elements of interest.

We propose that the dynamic and geometric characters of sandy bedforms can be summarized by four measures: a characteristic height, a characteristic length, a characteristic velocity, and a characteristic deformation. The first three have been computed by many different methods, but the last is, to the best of our knowledge, undeveloped. We will demonstrate here the use of two numeric functions, the roughness function and the cross-correlation function, that provide all four characteristic descriptors.

2 DATA

The field data used in the analyses presented here were collected with low-altitude aerial photography over the North Loup River in Nebraska (Mohrig, 1994). The 40 minute sequence of images obtained at 1 minute intervals was rectified with a grid of control points surveyed in the field. Bed elevations were calculated from the light intensity of the river bottom images by taking advantage of the attenuation of light through the water column. This process will be described in detail in future work.

The resulting data is a complete assessment of the bed, η, in four dimensions: x, y, z, & t, streamwise, cross-stream, vertical, and time, respectively. The grid resolution is 2cm x 2cm, and the rms horizontal positioning error from the rectification process is 10cm. The vertical resolution is 1mm, with a nominal accuracy of +/-2mm. The lengths along x & y are 31 and 15.5 meters respectively. For our purposes here, we are working with a single profile drawn from the middle of the bedform field. This profile has been detrended to remove the local mean bed elevation as well as a slight downstream shallowing.

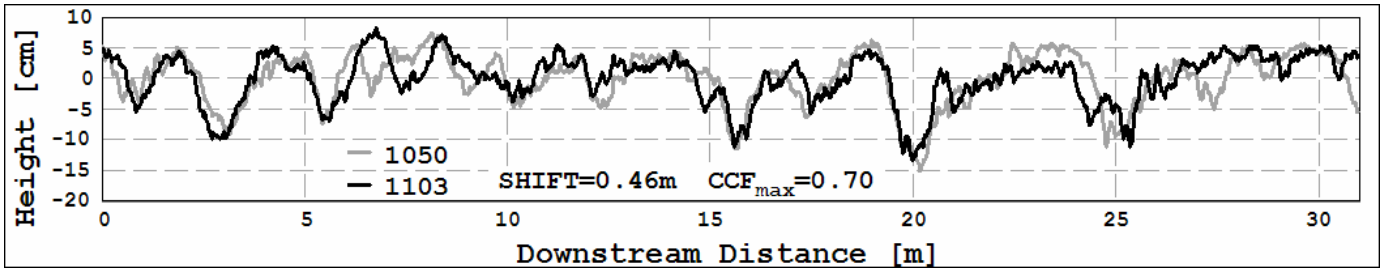

Figure 1. Two detrended bed-elevation profiles from North Loup River, one 13 minutes before the other. The evolved profile, 1103, is shifted relative to the initial profile, 1050, by the distance that results in the maximization of the cross-correlation function (CCF). Note that some regions show large fractions of direct overlap (translation dominant) while other regions exhibit very little overlap (deformation dominant). Flow is from left to right.

The data are therefore centered around zero but still express the original range of the bed elevation field (Fig. 1). The whole profile comprises about 10 dune scale bedforms and many smaller bedforms.

In addition data from the B2 flume experiment described by Blom and others (2003) is used. During that experiment longitudinal bed profiles were extracted from an evolving bed every 10 minutes. Resolution along a single profile is 1 cm and, and the velocity with which the instrument cart traveled was 15 cm/s. This differs from the field data, because the field photographs offer an actual instantaneous realization of the bed topography. In contrast, the experimental bed continued to evolve during the period over which each profile was collected. Dividing the total length, 28.3 m by 0.15 m/s gives a total collection time of approximately 3 minutes per profile. The effect of the continued evolution during the profile survey is that bed roughness elements in the profile appear expanded relative to their actual length. The manner in which this can be accounted for will be shown in the analyses that follow.

3 GEOMETRIC CHARACTER

The roughness function (Eq.1), the standard deviation of bed-elevation profile subsets, as a function of their length, produces a justifiable measure of the characteristic height and length for bed topography.

$$RF(\eta, L) = \sqrt{\frac{1}{N+1}\sum_{\phi=0}^{N}\sum_{x=\phi}^{\phi+L}[\eta(x)-\bar{\eta}(x)]^2} \qquad (1)$$

L is the variable length over which the roughness is calculated. N is the total number of windows of length L that exist in the profile domain, D, and $N+L=D$. This relation follows because the actual windowed subsets are not mutually exclusive. ϕ is the starting position along the profile of each window. It can be thought of like a phase position, and averaging over it gives the expected variance of the bed elevations as a function of L. The saturation roughness, RF_{sat}, is the value for the roughness function where it is no longer growing as a function of window size, L (Fig. 2). It is an approximation of the value that the roughness function asymptotically approaches, the standard deviation of the whole profile. The length scale associated with saturation, L_{sat}, could be defined in many ways. The most practical way is to define it as the window length, L, at which the slope of the plot in figure 2 is one-half that of the region with constant slope. It is closely related to the length scale that represents the largest bedforms. Through the use of analysis of regular forms, a sinusoid and a sawtooth pattern, McElroy and others (*in review*) show that the saturation roughness and length are related to the characteristic height and length by coefficients near unity. (Eq. 2; Eq. 3) The characteristic height and length capture the essence of bedform height and wavelength, respectively; they are the bulk statistical equivalent of traditional bedform picking methods.

The roughness-determined values of characteristic height and length are 0.11 m and 2.9 m, respectively, for the North Loup River example. These estimates are greater than the median values for height, 0.06 m, and length, 1.4 m, obtained via traditional measurement while in the field. Instead, the roughness-determined characteristic values correspond to the eighty-fifth percentile for all local measurements of the bedform topography and the ninety-fifth percentile for local measurements of bedform length.

$$H_c \cong 2.8RF_{sat} \quad (2)$$

$$L_c \cong 1.5L_{sat} \quad (3)$$

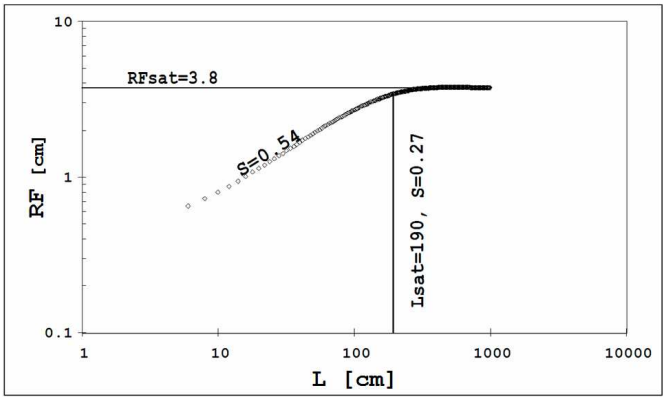

Figure 2. Roughness function for profile 1050 in figure 1. Saturation roughness and length are given as well as the slope of the constant slope region at lower window sizes, *L*.

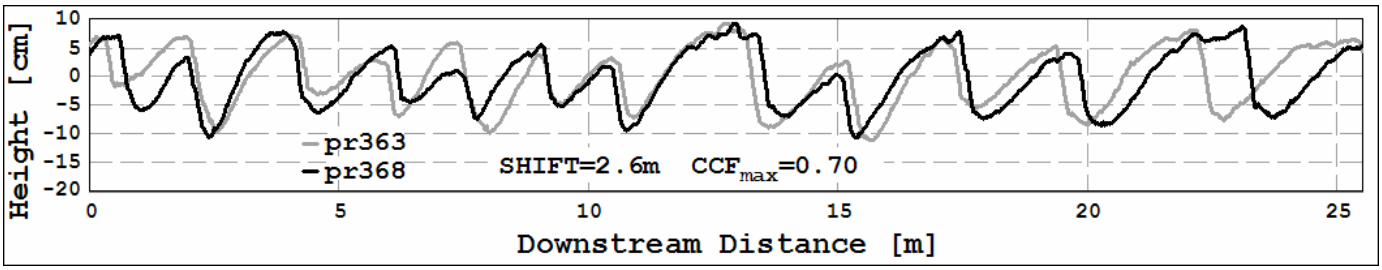

Figure 3. Two detrended bed-elevation profiles from B2 experiments (Blom et al., 2003), pr363 was collected 150 minutes before pr377. The evolved profile is shifted relative to the initial profile by the distance that results in the maximization of the cross-correlation function (CCF). Note that some regions show large fractions of direct overlap (translation dominant) while other regions exhibit very little overlap (deformation dominant). Flow is from left to right.

The difference between field and computed measurements suggests the bias of manual methods towards intermediate scales that is associated with unavoidable visual thresholds. It should be explicitly stated that the values determined in the field come from the very same surveyed reach that profile 1 represents. There is no doubt that traditional field methods underestimate the appropriate scales of size in the North Loup example.

For the B2 experimental data characteristic geometry, H_c=0.12 m and L_c=2.6 m. These values were calculated from analyses of 17 profiles that include those shown in figure 3. The characteristic length is an overestimate because of the effect of apparent expansion was not removed from the data. To do that, the characteristic velocity of the bed must be found. Essentially, the proportion of apparent compression is related to the rate of traversal of the instrument cart relative to the mean translational rate of the bed. (Eq. 4) Defining *f* as

$$f = 1 + \frac{v_{Bed}}{v_{Cart} - v_{Bed}} \quad (4)$$

the dilation factor, it can be seen that any bed feature of arbitrary length, *X*, traveling at a rate v_{Bed} in an observer's frame of reference will appear to have length *fX* in the frame of reference of an instrument cart traveling at velocity v_{Cart} relative to the observer's frame. The cart velocity is known, but the bed velocity, exactly the characteristic velocity, must be determined. In order to do this, we investigate the dynamic characteristics of the bed.

4 DYNAMIC CHARACTER

4.1 *Velocity*

Correlation can be used to quantify the evolution of a set bed profiles and has been used in both marine and fluvial settings (Duffy & Hughes-Clarke, 2005;

Nikora et al, 1997; McElroy & Mohrig, 2007). For an evolving bed, cross-correlation (Eq. 5; Davis, 1986) can used to estimate characteristic velocity by the relation between the mean bed translation and the duration of evolution (Fig 4).

$$CCF(L) = \frac{1}{N}\sum_{N}\frac{\eta_1(x)\times\eta_2(x+L)}{\sigma_1\sigma_2} \quad (5)$$

N is the number of elevation couples within the pair of profiles separated by the length, L. σ_1 and σ_2 are standard deviations of the two profile elevations. The distance of bed translation is taken to be the length that results in the maximization of the cross-correlation function. Linear regression of the relation between bed translation length and time interval yields a characteristic velocity, V_c (Eq. 6). For the field data, the characteristic velocity is 3.7 cm/min; it is the best fit for 40 minutes of evolution and can explain 99% of the covariance of translation length, L_T, and evolution duration, Δt.

$$L_T = V_c \Delta t \quad (6)$$

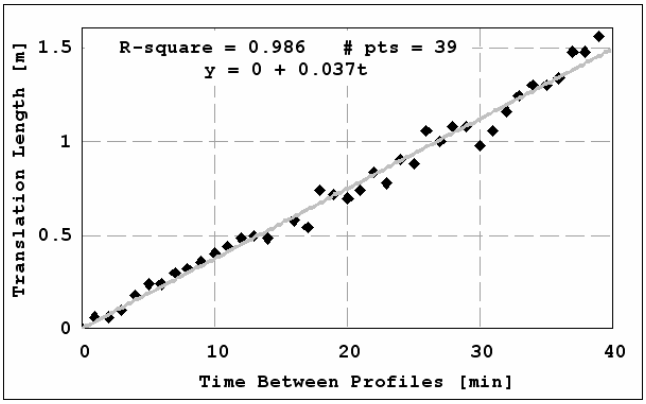

Figure 4. North Loup translation length as a function of bed evolution duration. Regression yields a characteristic velocity for the bed of 3.7cm/min and intercepts the origin.

The very high degree of goodness-of-fit for the characteristic velocity is due to the bed topography sample size and its resolution. Sample size is measured as the total length of the bed profile sample relative to the characteristic length of the bed, L_c, and the resolution is the distance between measurements relative to the characteristic length. For this data the total profile length is D=31m, and with L_c=2.9m, the sample size is approximate 10 characteristic bed lengths. Similarly, the elevation measurement spacing is Δx=2cm and therefore the resolution is ~150 measurements per characteristic length. We surmise that greater resolution and greater sample size both correspond to a more robust characteristic velocity estimate.

Characteristic velocity is found for the experimental data in the same manner but with one extra step because the measurements occur while the bed is evolving. Using Equation 6 coupled with the expression for the apparent dilation of the bed (Eq. 4), we determine a new relation to solve for the mean bed translation rate. (Eq. 7) Again, f is the dilation factor. Δt is the evolution duration, and $L_{T,App}$ is the apparent translation length. Because

$$V_c = \frac{1}{f}\frac{L_{T,App}}{\Delta t} \quad (7)$$

the characteristic velocity is defined as the velocity of the mean bed translation, V_c and v_{bed} are synonymous, and V_c appears on both sides of Equation 7. In this case, we can estimate the magnitude of the dilation factor as the slope of the plot in Figure 5 divided by the known velocity of the instrument cart. The result is a factor of approximately 0.5%. This means that all lengths were expanded by the measurement method by 5 parts in one thousand. For our purposes that can be neglected, and the uncorrected characteristic lengths and velocities can be accepted. This result is not general.

4.2 *Deformation*

We purport that deformation is the result of bed material transfer between bedforms and to a minor extent within bedforms. It is principally due to the emergence of small-scale topographic perturbations that grow to interact with the largest scale features and is manifest as changes in the shape, size, and relative spacing of bed topographic elements.

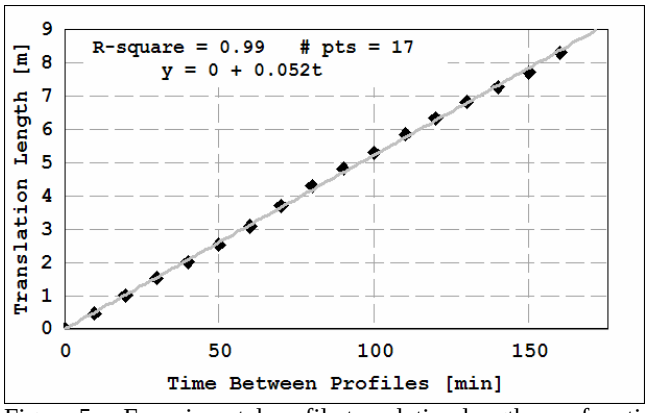

Figure 5. Experimental profile translation length as a function of bed evolution duration. Regression yields a characteristic velocity of 5.2cm/min and intercepts the origin.

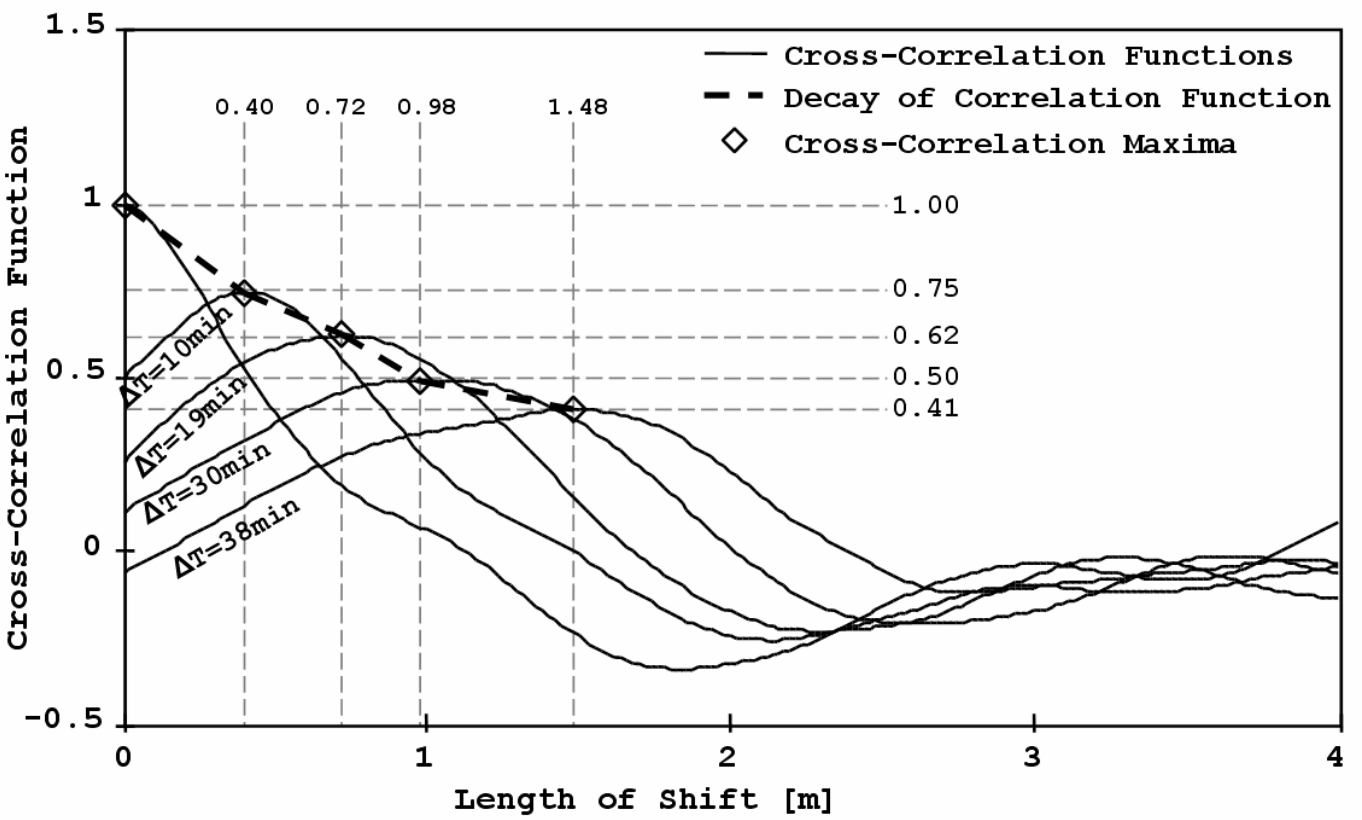

Figure 6. Cross-correlation functions (CCF) for a series of profiles from the North Loup data. Evolution durations are labeled as ΔT. The unlabeled CCF is the initial profile correlated with itself (autocorrelation). The maxima for the CCFs are associated with two other pieces of information: elapsed time between profiles and the shift lengths that result in maximization. Note that the CCF maxima decrease in magnitude but broaden in width during bed evolution.

As long as the amount of bed deformation is relatively minor, the translational length can still be estimated robustly as the shift length, L, that yields the maximum value for the CCF(L). At small translation lengths, deformation will similarly be slight, and the CCF will have a maximum value very near unity.

Characteristic deformation is determined by the secular decoupling of the bed from itself at some initial state. Specifically, the cross-correlation maximum decreases exponentially during bed evolution, and the region of highest correlation broadens (Fig. 6). The characteristic deformation is defined as the decay constant of the exponential relation. To make the relation general and to make the characteristic deformation comparable from system to system, the translation length must be normalized. The appropriate normalizing scale, the characteristic length, is used to create the dimensionless translation length, L_T^*. (Eq. 8)

$$L_T^* = \frac{L_T}{L_c} \tag{8}$$

In the North Loup data, the characteristic deformation is -1.7 and is a dimensionless quantity. (Fig. 7) This was determined by regression from the same 39 CCFs that represent total translation of just over half a characteristic length. This relation explains over 90% of the covariance between the CCF_{max} and L_T^*. A sediment-fluid, interfacial half-life can be defined as the value of dimensionless translation length required to drop the correlation of the evolved bed to its original state to a value of 50% (Eq. 9). Equation 9 shows the half-life of the bed is ~40% of a characteristic length:

$$\lambda = \frac{\ln(0.5)}{-1.8} = 0.39 \tag{9}$$

Over longer evolution durations, the magnitude of correlation decay cannot continue. This is due to an effective, non-zero, minimum similarity between two profiles that have the same statistical character. This behavior is not evident in our data because they represent a rather short dimensionless translation length.

The B2 experimental data, shown in Figure 8, have a characteristic deformation of -0.19. For the same 17 points used to determine the characteristic velocity, the exponential decay can explain over 90% of the covariance of the cross-correlation maxima and dimensionless translation lengths. The interfacial half life is λ=3.6.

5 DISCUSSION

Characteristic deformation in the flume is an order of magnitude lower than that of the field data. Even though the characteristic heights and lengths are within 10% of each other, characteristic velocities and deformations can be quite different. The velocities are within a factor of 1.5, but the difference in deformations implies a great distinction in process occurring between these two examples. One possibility that is visible by inspection of figures 1 and 3 is that the flume data have a paucity of secondary bedforms relative to the field data. These would accelerate small scale interactions and deformations that grow into larger-scale features that similarly interact.

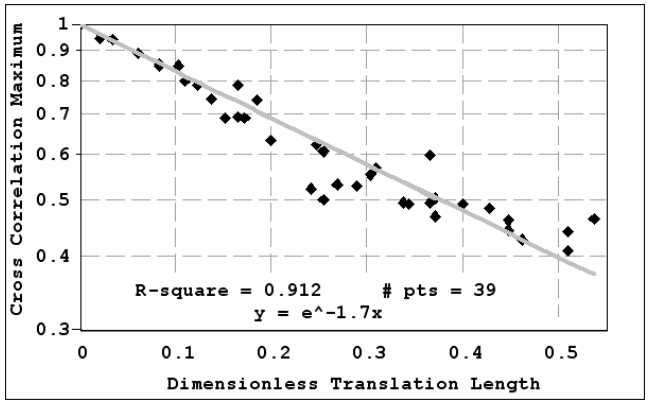

Figure 7. Decorrelation of North Loup bed profiles during evolution. Regression produces a characteristic deformation of -1.7. Expression for dimensionless translation length given by Equation 8.

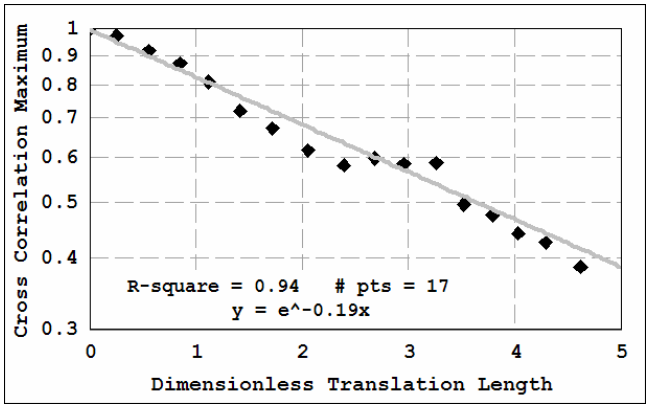

Figure 8. Decorrelation of experimental bed profiles during evolution. Regression produces a characteristic deformation of -0.19, an order of magnitude less than the field data.

Alternatively, the flume data represent conditions obtained in a well-controlled 2-dimensional flow environment while the field data are taken from a relatively uniform section of a fully 3-dimensional field environment. That likely means that the turbulent scales and intensities are much larger for the field data than for the flume data. Those two possibilities might very well be related and are certainly not exclusive nor representative of end-member conditions.

The process that results in the exponential nature of the correlation decay has an important statistical interpretation. As the bed evolves from the transport of material, the topography demonstrates two major behaviors, translation and deformation. While the translation can be thought of as the displacement of kinematic waves, the deformation can be cast as being an injection of new information into the bed that had not been present before. The exponential nature of the decay suggests that the new information added at each step is in constant proportion to the total information content of the bed. In other words, at each time step the bed is constituted by some percent of its previous state and by some percent of that new information. As long as flow conditions are consistent, then the relative dependence upon the previous state, memory, is constant. The memory, *m*, is defined as the compliment of the decay after being discretized and normalized, i.e. *m*=83% per 0.1 L_T^* in the North Loup case and m=98% per 0.1 L_T^* in the B2 experimental case. As in the example, *m* is a function of the dimensionless translation length used for discretizing. The memory has a relation to the bed flux responsible for deformation that we are currently examining.

6 FINAL REMARKS

We have shown methods for computationally obtaining four characteristic scales of bed topography, height, length, velocity and deformation, from two mathematical measures, the roughness function and cross-correlation. These will have great applicability across a range of conditions, and measurement techniques. Specifically, a manner for deducing the relative importance of bed evolution during a survey has been presented and shown in our laboratory case to be negligible. We hope that these methods will be found robust and useful for acoustically derived data

-especially because these methods will make it possible to analyze the great abundance of data that can be collected in one survey period. Finally, these characteristic properties make ideal candidates for measures that can be used to compare rivers across scales.

REFERENCES

Blom, A., Ribberink, J., de Vriend, H. 2003. Vertical sorting of bed forms: flume experiments with a natural and a tri-modal sediment mixture, *Water Resources Research*, v. 39, p. 1025.

Davis, J. 1986. *Statistics and Data Analysis in Geology*. Wiley & Sons, New York, 646pp.

Duffy, G., Hughes-Clarke, J. 2005. Application of spatial cross correlation to detection of migration of submarine sand dunes, *Journal of Geophysical Research*, v.110, F04S12.

Hino, M. 1968. Equilibrium-range spectra of sand waves formed by flowing water, *Journal of Fluid Mechanics*, v. 34, p. 565-573.

Jerolmack, D., & Mohrig, D. 2005a. A unified model for subaqueous bed form dynamics, *Water Resources Research*, v. 41, W12421.

Jerolmack, D., & Mohrig, D. 2005b. Interactions between bed forms: Topography, turbulence and transport, *Journal of Geophysical Research- Earth Surface*, v. 110, F02014.

McElroy, B., Mohrig, D. 2007. Correlation decay and dynamic equilibrium in sandy transport systems, *Conference proceedings*: *River, Coastal, and Estuarine Morphodynamics 2007*.

McElroy, B., Mohrig, D., Jerolmack, D. *in review*. Quantifying topographic roughness in sandy transport systems, *Geophysical Research Letters*.

Mohrig, D. 1994 Spatial evolution of dunes in a sandy river, doctoral dissertation, University of Washington, 119pp.

Nikora, V., Sukhodolov, A., Rowinski, P. 1997. Statistical sand wave dynamics in one-directional water flows, *Journal of Fluid Mechanics*, v. 351, p. 17-39.

Nordin, C. 1971. Statistical properties of dune profiles, *United States Geologic Survey Professional Paper*, 562-F, 41pp.